How to cite: Angew. Chem. Int. Ed. **2020**, 59, 17172–17176
International Edition: doi.org/10.1002/anie.202002280
German Edition: doi.org/10.1002/ange.202002280

Atomic Layer Deposition

Atomic Layer Deposition of Cobalt Phosphide for Efficient Water Splitting

*Haojie Zhang, Dirk J. Hagen, Xiaopeng Li, Andreas Graff, Frank Heyroth, Bodo Fuhrmann, Ilya Kostanovskiy, Stefan L. Schweizer, Francesco Caddeo, A. Wouter Maijenburg, Stuart Parkin, and Ralf B. Wehrspohn**

Abstract: *Transition-metal phosphides (TMP) prepared by atomic layer deposition (ALD) are reported for the first time. Ultrathin Co-P films were deposited by using PH_3 plasma as the phosphorus source and an extra H_2 plasma step to remove excess P in the growing films. The optimized ALD process proceeded by self-limited layer-by-layer growth, and the deposited Co-P films were highly pure and smooth. The Co-P films deposited via ALD exhibited better electrochemical and photoelectrochemical hydrogen evolution reaction (HER) activities than similar Co-P films prepared by the traditional post-phosphorization method. Moreover, the deposition of ultrathin Co-P films on periodic trenches was demonstrated, which highlights the broad and promising potential application of this ALD process for a conformal coating of TMP films on complex three-dimensional (3D) architectures.*

H_2, owing to its high gravimetric energy density (142 MJ kg^{-1}) and zero-carbon emission, has been regarded as an ideal energy carrier for clean and sustainable energy storage and supply to meet the serious global energy crisis and environmental pollution.[1] Pt-based components form the state-of-the-art electrocatalysts for the hydrogen evolution reaction (HER) and exhibit excellent catalytic activity in electrolytes with a wide pH-range.[2] However, the scarcity and high costs of Pt seriously restrict their large-scale commercialization. Therefore, enormous research efforts are focused on developing alternatives for Pt-based electrocatalysts, such as carbon-based materials, sulfides, selenides, nitrides and phosphides, to reduce the costs for efficient water splitting.[3] Among these candidates, transition-metal phosphides (TMP) have attracted increasing research interest due to their excellent performance, various crystalline phases, and tunable electronic structure.[4] Inspired by this, various strategies have been employed to prepare TMP-based electrocatalysts, including the solvent-phase method, the solid-state method, the gas-solid method, and the electrodeposition method.[5] For example, Jiang et al. prepared cobalt-phosphorous-derived Co-P films on Cu foil by electrodeposition, exhibiting remarkable bifunctional activities for both the HER and the oxygen evolution reaction (OER).[6] Jaramillo and co-workers combined CoP thin films with Si photo-absorbers to prepare highly efficient precious metal-free crystalline silicon photocathodes by an evaporation-phosphorization process.[7] Recently, Li et al. synthesized P-rich CoP_2 via a hot-injection method, exhibiting excellent electrochemical activities for the HER.[8] However, the controllable and homogeneous deposition of an ultrathin TMP film on complex three-dimensional (3D) structures is still a great challenge.

Atomic layer deposition (ALD) has become a powerful technology for the preparation of high-quality thin-film materials on various complex substrates.[9] ALD is a surface self-limited and saturated deposition process enabling the layer-by-layer and large-scale deposition of uniform and reproducible films. Due to this specific advantage, ALD is suitable for depositing homogeneous coatings on various

[*] H. Zhang, Dr. S. L. Schweizer, Prof. R. B. Wehrspohn
Institute of Physics
Martin Luther University Halle-Wittenberg
Heinrich-Damerow-Strasse 4, 06120 Halle, Saale (Germany)
E-mail: ralf.wehrspohn@physik.uni-halle.de

Dr. D. J. Hagen, Dr. I. Kostanovskiy, Prof. S. Parkin
Max Planck Institute of Microstructure Physics
Weinberg 2, 06120 Halle, Saale (Germany)

Prof. X. Li
State Key Laboratory for Modification of Chemical Fibers and Polymer Materials & College of Materials Science and Engineering, Donghua University
Shanghai 201620 (China)

Dr. A. Graff
Fraunhofer Institute for Microstructure of Materials and Systems
Walter-Hülse-Strasse 1, Halle, Saale (Germany)

Dr. F. Heyroth, Dr. B. Fuhrmann
Interdisciplinary center of materials science, Martin Luther University Halle-Wittenberg
Heinrich-Damerow-Strasse 4, 06120 Halle, Saale (Germany)

Dr. F. Caddeo, Prof. A. W. Maijenburg
Centre for Innovation Competence SiLi-nano®, Martin Luther University Halle-Wittenberg
Karl-Freiherr-von-Fritsch-Strasse 3, 06120 Halle, Saale (Germany)

Prof. R. B. Wehrspohn
Fraunhofer-Gesellschaft
Hansastrasse 27 c, 80686 Munich, (Germany)

Supporting information and the ORCID identification number(s) for the author(s) of this article can be found under: https://doi.org/10.1002/anie.202002280.

© 2020 The Authors. Published by Wiley-VCH GmbH. This is an open access article under the terms of the Creative Commons Attribution Non-Commercial License, which permits use, distribution and reproduction in any medium, provided the original work is properly cited, and is not used for commercial purposes.

complex 3D structures, thus exhibiting a huge potential in various applications (e.g. microelectronics and catalysis). Up to now, no ALD-process for the direct deposition of TMP was reported and only a few publications reported the preparation of TMP films by post-treatment of ALD-grown films. For example, Rongé et al. used ALD for the deposition of metal phosphates (M = Co and Fe), which were subsequently reduced by thermal annealing in a reducing environment (H_2) or electrochemical treatment for the preparation of metal phosphides.[10] However, the high-temperature annealing (950 °C) resulted in the formation of particulate films, while the ability of the electrochemical treatment to reduce the complete film remains doubtful. Looking for suitable chemistry for TMP-ALD processes, it is worth noticing recent advances in the ALD of transition metal sulfides. Guo et al. reported a universal ALD process to deposit pyrite-type metal disulfides (FeS_2, CoS_2, and NiS_2).[11] The well-crystallized films prepared with optimized ALD recipes could be uniformly deposited even into deep, narrow trenches with high aspect ratios.

Probably, the main reason for the unsuccessful development of an ALD recipe for the deposition of TMP so far is the serious decomposition of PH_3 during the PH_3 plasma treatment step in the standard ALD process, which leads to an excess content of phosphorus (P) residing in the deposited layer.[12] The excess P, which cannot be eliminated in the subsequent Ar purge step, would continue to react with the precursor, thus leading to an uncontrollable deposition.[13] Gudovskikh et al. studied the deposition process of GaP in a chemical vapor deposition (CVD) system by in situ optical emission spectroscopy (OES).[13] They found that the presence of traces of PH_3, which comes from the reaction of H_2 and P species on the chamber wall, can significantly affect the deposition process and that an additional H_2 plasma step effectively removed the P species on the chamber wall, resulting in a reduced growth rate and a more homogeneous deposition. A "third" H_2 or H_2 plasma step was also successfully applied in various ALD processes to obtain the desired stoichiometry. For example, Mackus et al. used H_2 or H_2 plasma to reduce PtO_x to Pt in room temperature ALD processes employing $(Me)_3Pt(MeCp)$ and O_2 plasma as precursor-reactant pair.[14] Similar combinations of oxidizing and reducing reagents have also been employed for the deposition of Ir,[15] Co,[16] and Cu.[17] Therefore, an additional step to remove the excess P is the key to obtain a self-limited and layer-by-layer deposition of TMP-based catalysts via ALD.

Herein, we report a plasma-assisted ALD process for depositing ultrathin Co-P films using PH_3 plasma and bis(N-*t*-butyl-*N′*-ethylpropanimidamidato) cobalt(II) ($Co(AMD)_2$) as the phosphorus source and metal precursor, respectively. In addition, an H_2 plasma step was employed during the deposition to remove excessive phosphorus. The optimized recipe followed the ideal layer-by-layer ALD growth behavior over a wide temperature range, resulting in pure and stable polycrystalline Co-P films. The electrodes prepared by depositing such Co-P films on fluorine-doped tin oxide (FTO) glass and p-type Si wafer, exhibited improved electrochemical and photoelectrochemical HER activities in alkaline electrolyte when compared to that of Co-P films prepared by a conventional post-phosphorization method. Furthermore, we demonstrate that the ALD Co-P can be conformally deposited into deep Si trenches, highlighting the promising potential application of depositing TMP on complex 3D architectures.

The controllable deposition of stable Co-P ultrathin films by ALD was conducted at a pressure of 100 mtorr with the assistance of PH_3 (3% in Ar) plasma and H_2 plasma as illustrated in Figure 1. Planar Si wafers with a native oxide layer (SiO_x) were used as substrates to study and optimize the deposition behavior of Co-P. This procedure induced a saturated growth process which was demonstrated by varying the exposure time of the metal precursor (t_1) and the PH_3 plasma (t_2) at a substrate temperature of 265 °C (Figure 2a,b). Figure 2a reveals that the growth rate increases initially with the increase of t_1 until saturation is achieved as t_1 exceeding approximately 3 s at fixed t_2 (5 s) and H_2 plasma time (t_3 = 10 s). Similarly, while fixing t_1 at 3 s, the growth rate

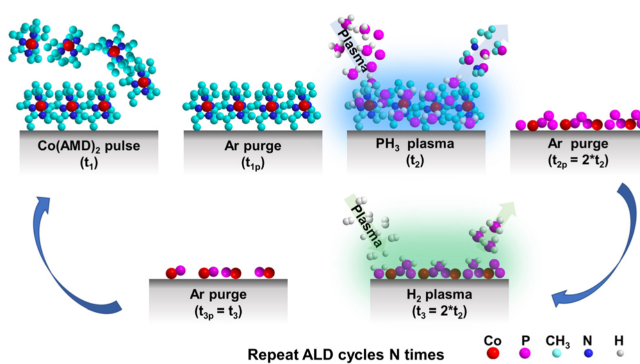

Figure 1. Illustration of the plasma-enhanced ALD process for the deposition of Co-P films.

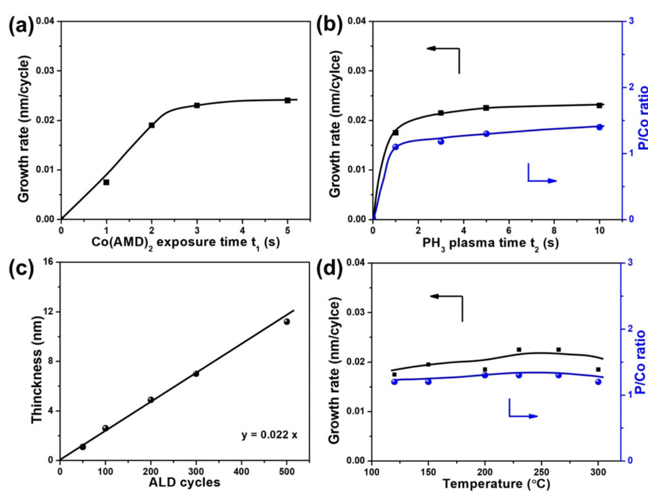

Figure 2. Exploration of Co-P ALD process a) Growth rates versus the metal-precursor exposure time at fixed t_2 (5 s) and H_2 plasma time t_3 (10 s). b) Growth rates and their corresponding P/Co atomic ratios of prepared Co-P films versus PH_3 plasma treatment time at constant t_1 (3 s). c) Thickness of deposited Co-P films as a function of total number of ALD cycles. d) Temperature dependency of the growth rates and the P/Co ratios.

 © 2020 The Authors. Published by Wiley-VCH GmbH

increased firstly with increasing t_2 and then reached saturation as t_2 exceeding approximately 5 s (Figure 2b). The impact of the H_2 plasma step was also investigated by changing its length from $t_3 = 0$ to $t_3 = 3*t_2$. As shown in Figure S1 in the Supporting Information, the saturation of the growth rate and P/Co ratio was achieved when $t_3 \geq 2*t_2$. Thus, the H_2 plasma does not etch the Co-P film further. Rutherford backscattering spectrometry (RBS) revealed that the ratio of P/Co is approximately 1.3 under the saturated growth rate condition. These results indicate that the self-limited layer-by-layer deposition behavior was achieved with sufficient exposure of $Co(AMD)_2$ and PH_3 plasma. Therefore, the saturated condition of $t_1 = 3$ s, $t_2 = 5$ s and $t_3 = 10$ s were used as a standard recipe for the deposition of Co-P films if not mentioned otherwise. Figure 2c shows that the thickness of the deposited Co-P films has a linear relationship with the number of ALD cycles with a slope of 0.022 nm/cycle under the standard recipe conditions, indicating a controllable deposition behavior. For the comparison, Co-P films deposited without the assistance of H_2 plasma demonstrated an uncontrollable deposition behavior with a high growth rate of 0.16 nm/cycle. RBS revealed that the as-deposited Co-P film deposited without H_2 plasma exhibited a high P content (P/Co = 3.5). Moreover, the as-deposited Co-P film was not stable and was easily oxidized to phosphates in the air (Figure S2). Therefore, the following reactions may happen during the H_2 plasma step [Eqs. (1)–(2)]:[13]

$$H_2 + e \rightarrow H + H^* + e \quad (1)$$

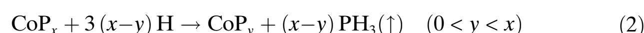

$$CoP_x + 3(x-y)H \rightarrow CoP_y + (x-y)PH_3(\uparrow) \quad (0 < y < x) \quad (2)$$

Next, the influence of the temperature on the deposition of Co-P films was investigated. As shown in Figure 2d, the deposition process exhibited a wide temperature window from 120 to 300 °C with an almost constant growth rate. Moreover, RBS revealed that the deposited films exhibited an almost constant P/Co ratio (Figure 2d). The precursor decomposition was also investigated by only pulsing $Co(AMD)_2$ at 265 °C without PH_3 and H_2 plasma steps (denoted as $Co(AMD)_2$-decom./Si). X-ray photoelectron spectroscopy (XPS) measurements indicate that only a small amount of Co (5.59 atomic %) is present on the substrate surface (Figure S3(a–c)) after 200 cycles, which is consistent with a molecular monolayer, which probably decomposed after exposure to the air. The XPS profile (Figure S3(d)) further reveals that there is no obvious layer on the substrate, indicating that there is negligible precursor decomposition at 265 °C, which has little impact on the ALD process. Nevertheless, we focus on the characterization of Co-P films deposited at 265 °C in the following.

The morphology of the deposited Co-P films was characterized by transmission electron microscopy (TEM). As shown in Figure 3(a), the top-view TEM image of the Co-P film deposited on an amorphous SiN_x membrane with 300 cycles (6.7 nm) revealed that the as-deposited film exhibits regions of high crystallinity and regions of amorphous material. The region with high crystallinity demonstrates a lattice spacing of 0.25 nm, which can be associated with the (200) facet of CoP (PDF#29-0497).[18] The cross-section view of Co-P films deposited on Si (Figure 3b) also indicates the polycrystalline property with crystal lattices of 0.28, 0.20, and 0.19 nm which can be associated to the (011), (210), and (211) facets of CoP, respectively. The electron diffraction pattern (Figure 3a) indicates that the main crystal structure of the Co-P film is associated with the crystal structure of CoP, which is consistent with the HRTEM results. Furthermore, similar morphology and crystalline phase are obtained for Co-P films deposited at 125 °C (Figure S4(a,b)) highlighting the wide temperature window for our process. The energy-dispersive X-ray spectroscopy (EDS) mapping of the Co-P films further revealed the high quality of the deposited layer (Figure 3b, inset). Strong O signals are only observed at the surface of the Co-P films and its interface with the Si substrate, which can be assigned to the formation of a surface oxide due exposure to air (or adsorbed O_2/H_2O species) and the native oxide layer of the Si wafer. An optical photograph of one piece of Co-P/Si (6.7 nm Co-P) and the corresponding atomic force microscopy (AFM) measurement (Figure 3c) indicate that the deposited films are fairly smooth with a roughness of 0.37 nm.

The purity of the deposited Co-P films was also characterized by XPS. The depth profile of the deposited Co-P films (Figure 3d) indicates that they are pure with negligible N, C, and O contaminations. The surface O species were also detected, which is consistent with the EDS mapping. The Co 2p spectrum (Figure 3e) acquired from the surface of the Co-P films shows a pair of spin-orbit split peaks at 778.8 eV (Co $2p_{3/2}$) and 793.8 eV (Co $2p_{1/2}$), which are characteristic peaks of CoP.[19] In addition, the P 2p spectrum Figure 3f shows doublet peaks at 129.4 eV (P $2p_{3/2}$) and 130.3 eV (P $2p_{1/2}$) and an extra peak at 133.1 eV, which correspond to Co–P

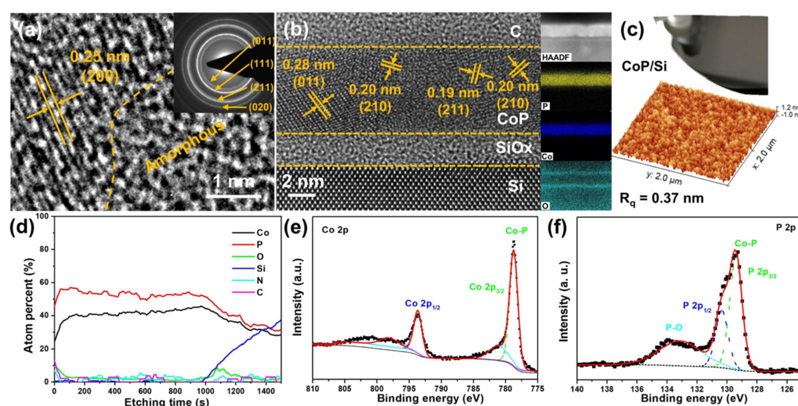

Figure 3. Structural and compositional analysis of Co-P films deposited at 265 °C. TEM images of a) top view of Co-P film deposited on amorphous SiN_x membrane and the electron diffraction pattern of a thicker films (25 nm) as shown in inset. b) cross-section view of Co-P film deposited on Si at 265 °C with the corresponding EDS mapping (inset). c) Optical photograph of one piece of Co-P/Si and the corresponding AFM measurement. d) XPS profile of a Co-P film with a thickness of 25 nm. e),f) XPS spectra of Co-P/Si for e) Co 2p and f) P 2p.

© 2020 The Authors. Published by Wiley-VCH GmbH

and P–O bonds, respectively. Furthermore, similar spectra were obtained for Co 2p and P 2p after storage for around 3 months in the ambient environment, indicating good stability and resistance to oxidation in air (Figure S5). It should be mentioned that a stronger O signal is observed on the surface of Co-P films, but the inner layer of Co-P still contains no O (Figure S6) which indicates that the O species on the surface of Co-P films increase slowly with the storage time and provide protection against oxidation of the film bulk which is in sharp contrast to the Co-P films deposited without the H_2 plasma step.

The HER activity of the Co-P films prepared with our ALD process was assessed by depositing Co-P films on an FTO glass substrate, and the corresponding optical photograph is shown in Figure S7. As shown in Figure 4a, the sample labeled as Co-P/FTO, which was fabricated by depositing 6.7 nm Co-P on FTO at 265 °C using our optimized ALD recipe, demonstrates a significantly enhanced HER performance compared to bare FTO and Co-P/FTO-thermal which was prepared by the traditional thermal post-phosphorization of CoO_x (10 nm) deposited by ALD on FTO.[19] The as-prepared Co-P/FTO electrode requires an overpotential of 254 mV to deliver a current density of 10 mA cm^{-2} (η_{10}), which is much lower than that of bare FTO (η_{10} = 663 mV) and Co-P/FTO-thermal (η_{10} = 320 mV) but still higher than that of Pt/FTO (η_{10} = 105 mV). Figure 4b shows that Co-P/FTO exhibits better reaction kinetics with a smaller Tafel slope of 59 mV dec^{-1} than that of bare FTO (253 mV dec^{-1}) and Co-P/FTO-thermal (95 mV dec^{-1}). Electrochemical impedance spectroscopy (EIS) measurements were also employed to investigate the reaction mechanisms (Figure 4c and Table S1), and the related results were fitted with the equivalent circuit as shown in the inset of Figure 4c. The EIS results reveal that Co-P/FTO exhibits a smaller charge transfer resistance (R_{ct} = 22.8 Ω) than Co-P/FTO-thermal (R_{ct} = 69.5 Ω), suggesting facilitated electron transfer for HER.[20] The thickness-dependent HER activities of Co-P/FTO are also investigated. As shown in Figure S8, an optimized performance is achieved with an approximately 6.7 nm Co-P film. The electrochemical surface area (ECSA) measurement indicates that Co-P/FTO with a higher capacitance (C_{dl}) has more accessible active sites than CoP/FTO-thermal (Figure S9). The turnover frequency (TOF) for Co-P/FTO is estimated to be 0.08 s^{-1} (η = 100 mV), which is higher than that of other cathodes reported in the literature (Table S2).[8,21] Furthermore, the as-prepared Co-P/FTO electrode exhibited good stability over an examination time of 36 h (Figure 4d) at a current density of 10 mA cm^{-2}. Next, Co-P films deposited on p-B Si wafer (Co-P/Si) were evaluated for photoelectrochemical water splitting, which shows that the Co-P/Si demonstrates a better photoelectrochemical HER performance than that of the Co-P/Si-thermal (Figure 4e). It can be observed that the Co-P/Si demonstrates a more positive onset potential (0.27 V) than the Co-P/Si-thermal (−0.18 V), which is defined as the required potential for achieving a current density of −0.1 mA cm^{-2}. A saturated photocurrent of around 32 mA cm^{-2} is achieved by Co-P/Si, which is higher than other reports (Table S3).[7,8,22] The virtually instantaneous photoresponse for Co-P/Si under chopped light irradiation (Figure 4f) reveals that our deposited Co-P films have the potential to be used as the cocatalyst to improve the photoelectrochemical activity of semiconductors.

We also evaluated the coverage ability of the ALD process by depositing Co-P films into deep-narrow Si trenches (Figure 5a). By comparing with the bare Si trenches (Figure S10), it can be seen that the Co-P films conformally cover the trenches (Figure 5b,c). These results clearly reveal the

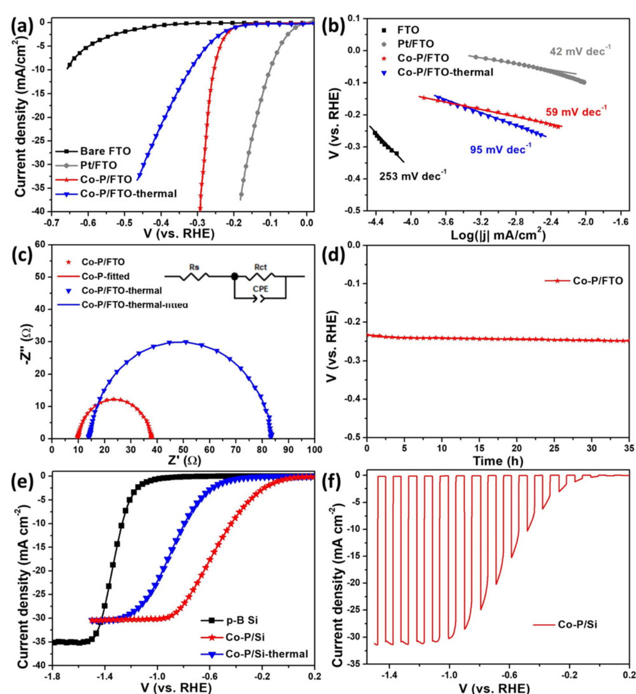

Figure 4. a) LSV curves of the prepared Co-P/FTO, Co-P/FTO-thermal, Pt/FTO and bare FTO electrodes for HER in 1 M KOH. b),c) The corresponding Tafel and EIS measurements of the prepared electrodes. The corresponding equivalent circuit for the EIS fitting is shown in the inset of (c), where R_s is the ohmic resistance, R_{ct} is the charge transfer resistance, and CPE is the constant phase element. d) Long-time measurement of the prepared Co-P/FTO for HER acquired at 10 mA cm^{-2}. e) LSV curves of the prepared Co-P/Si, Co-P/Si-thermal and p-B Si for photoelectrochemical HER in 1 M KOH with the illumination of a solar simulator. f) Transient photocurrent responses to chopped light irradiation of Co-P/Si.

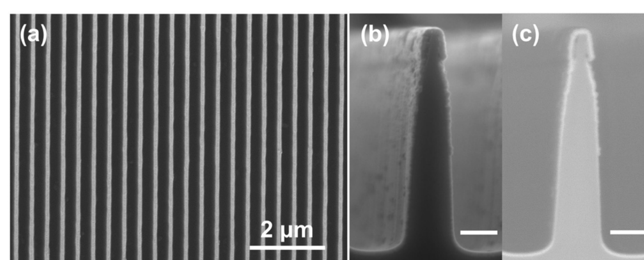

Figure 5. a) Top view of Co-P coated Si trenches. b) Cross-section view secondary-electron (SE) SEM image and c) the corresponding back-scattered-electron (BSE) image of conformally coated Si trenches with Co-P films. The scale bars in (b) and (c) are 200 nm.

 © 2020 The Authors. Published by Wiley-VCH GmbH

homogenous coating ability of our ALD process, and further indicate the promising potential application of a conformal coating of ultrathin Co-P films on complex 3D structures.

In summary, we reported a new ALD process for the preparation of ultrathin Co-P films with the assistance of H_2 plasma to remove the excess phosphorus during each ALD cycle. The optimized ALD process proceeds by a self-limited layer-by-layer deposition to produce high quality and smooth Co-P films. The as-prepared Co-P films on FTO glass and Si demonstrate enhanced electrochemical and photoelectrochemical HER activities than that of Co-P/FTO-thermal prepared by a post-phosphorization method. Furthermore, the Co-P films can be conformally deposited into periodic Si trenches, highlighting the capacity for controllable and conformal coating of Co-P films on complex 3D structures.

Acknowledgements

We thank Dr. Bodo Kalkofen, Dr. Dirk Sander and Dr. Fang Gao for their help with the maintenance of the ALD system and Dr. Sara Azimi for her help to improve the ALD system at the Max Planck Institute of Microstructure Physics. We also acknowledge Dr. Felix Börrnert for the assistance of TEM measurement at MPI. The financial support by the BMBF-project Struktursolar is highly acknowledged. X. L. acknowledges the financial support from the National Science Foundation of China (Grant No. 21972163), the Fundamental Research Funds for the Central Universities and the DHU Distinguished Young Professor Program. Open access funding enabled and organized by Projekt DEAL.

Conflict of interest

The authors declare no conflict of interest.

Keywords: atomic layer deposition (ALD) · PH_3 plasma · thin-films · transition-metal phosphide (TMP) · water splitting

[1] a) S. Chu, A. Majumdar, *Nature* **2012**, *488*, 294; b) S. E. Hosseini, M. A. Wahid, *Renewable Sustainable Energy Rev.* **2016**, *57*, 850; c) L. Schlapbach, A. Züttel, *Nature* **2001**, *414*, 353.

[2] a) R. Subbaraman, D. Tripkovic, D. Strmcnik, K.-C. Chang, M. Uchimura, A. P. Paulikas, V. Stamenkovic, N. M. Markovic, *Science* **2011**, *334*, 1256; b) N. Cheng, S. Stambula, D. Wang, M. N. Banis, J. Liu, A. Riese, B. Xiao, R. Li, T.-K. Sham, L.-M. Liu, et al., *Nat. Commun.* **2016**, *7*, 13638.

[3] a) S. Sultan, J. N. Tiwari, A. N. Singh, S. Zhumagali, M. Ha, C. W. Myung, P. Thangavel, K. S. Kim, *Adv. Energy Mater.* **2019**, *9*, 1900624; b) H. Sun, Z. Yan, F. Liu, W. Xu, F. Cheng, J. Chen, *Adv. Mater.* **2019**, *31*, 1806326; c) X. Du, J. Huang, J. Zhang, Y. Yan, C. Wu, Y. Hu, C. Yan, T. Lei, W. Chen, C. Fan, et al., *Angew. Chem. Int. Ed.* **2019**, *58*, 4484; *Angew. Chem.* **2019**, *131*, 4532; d) J. Li, R. Güttinger, R. Moré, F. Song, W. Wan, G. R. Patzke, *Chem. Soc. Rev.* **2017**, *46*, 6124.

[4] J. Joo, T. Kim, J. Lee, S.-I. Choi, K. Lee, *Adv. Mater.* **2019**, *31*, 1806682.

[5] a) J. F. Callejas, C. G. Read, C. W. Roske, N. S. Lewis, R. E. Schaak, *Chem. Mater.* **2016**, *28*, 6017; b) Y. Wang, B. Kong, D. Y. Zhao, H. T. Wang, C. Selomulya, *Nano Today* **2017**, *15*, 26; c) G. Zhao, K. Rui, S. X. Dou, W. Sun, *Adv. Funct. Mater.* **2018**, *28*, 1803291; d) M. Sun, H. Liu, J. Qu, J. Li, *Adv. Energy Mater.* **2016**, *6*, 1600087; e) H. Zhang, A. W. Maijenburg, X. Li, S. L. Schweizer, R. B. Wehrspohn, *Adv Funct. Mater.* **2020**, https://doi.org/10.1002/adfm.202003261.

[6] N. Jiang, B. You, M. L. Sheng, Y. J. Sun, *Angew. Chem. Int. Ed.* **2015**, *54*, 6251; *Angew. Chem.* **2015**, *127*, 6349.

[7] T. R. Hellstern, J. D. Benck, J. Kibsgaard, C. Hahn, T. F. Jaramillo, *Adv. Energy Mater.* **2016**, *6*, 1501758.

[8] H. Li, P. Wen, D. S. Itanze, M. W. Kim, S. Adhikari, C. Lu, L. Jiang, Y. Qiu, S. M. Geyer, *Adv. Mater.* **2019**, *31*, 1900813.

[9] a) S. Sharma, J. Waldman, S. Afshari, B. Fekete, *Renewable Sustainable Energy Rev.* **2019**, *101*, 112; b) B. C. Mallick, C.-T. Hsieh, K.-M. Yin, Y. A. Gandomi, K.-T. Huang, *ECS J. Solid State Sci. Technol.* **2019**, *8*, N55–N78.

[10] J. Rongé, T. Dobbelaere, L. Henderick, M. M. Minjauw, S. P. Sree, J. Dendooven, J. A. Martens, C. Detavernier, *Nanoscale Adv.* **2019**, *1*, 4166.

[11] Z. Guo, X. Wang, *Angew. Chem. Int. Ed.* **2018**, *57*, 5898; *Angew. Chem.* **2018**, *130*, 6000.

[12] G. Bruno, P. Capezzuto, M. Losurdo, *J. Phys. IV* **1995**, *05*, C5-481-C5-488.

[13] A. V. Uvarov, A. S. Gudovskikh, *J. Phys. Conf. Ser.* **2018**, *1038*, 012108.

[14] A. J. M. Mackus, D. Garcia-Alonso, H. C. M. Knoops, A. A. Bol, W. M. M. Kessels, *Chem. Mater.* **2013**, *25*, 1769.

[15] J. Hämäläinen, E. Puukilainen, M. Kemell, L. Costelle, M. Ritala, M. Leskelä, *Chem. Mater.* **2009**, *21*, 4868.

[16] M. Daub, M. Knez, U. Goesele, K. Nielsch, *J. Appl. Phys.* **2007**, *101*, 09J111.

[17] T. S. Tripathi, M. Karppinen, *Chem. Mater.* **2017**, *29*, 1230.

[18] L. Su, X. Cui, T. He, L. Zeng, H. Tian, Y. Song, K. Qi, B. Y. Xia, *Chem. Sci.* **2019**, *10*, 2019.

[19] H. J. Zhang, X. P. Li, A. Hahnel, V. Naumann, C. Lin, S. Azimi, S. L. Schweizer, A. W. Maijenburg, R. B. Wehrspohn, *Adv. Funct. Mater.* **2018**, *28*, 1706847.

[20] S. Song, M. Guo, S. Zhang, K. Zhan, Y. Yan, J. Yang, B. Zhao, M. Xu, *Electrochim. Acta* **2020**, *331*, 135431.

[21] a) R. Zhang, X. Wang, S. Yu, T. Wen, X. Zhu, F. Yang, X. Sun, W. Hu, *Adv. Mater.* **2017**, 29, 1605502; b) E. J. Popczun, J. R. McKone, C. G. Read, A. J. Biacchi, A. M. Wiltrout, N. S. Lewis, R. E. Schaak, *J. Am. Chem. Soc.* **2013**, *135*, 9267; c) E. J. Popczun, C. G. Read, C. W. Roske, N. S. Lewis, R. E. Schaak, *Angew. Chem. Int. Ed.* **2014**, *53*, 5427; *Angew. Chem.* **2014**, *126*, 5531.

[22] a) J. Zhao, L. Cai, H. Li, X. Shi, X. Zheng, *ACS Energy Lett.* **2017**, *2*, 1939; b) S. M. Thalluri, J. Borme, K. Yu, J. Y. Xu, I. Amorim, J. Gaspar, L. Qiao, P. Ferreira, P. Alpuim, L. F. Liu, *Nano Res.* **2018**, *11*, 4823.

Manuscript received: April 13, 2020
Accepted manuscript online: June 30, 2020
Version of record online: August 7, 2020

© 2020 The Authors. Published by Wiley-VCH GmbH